AAPS PharmSciTech (2026) 27:42
https://doi.org/10.1208/s12249-025-03261-x

RESEARCH ARTICLE

Development and *In Vivo* Evaluation of QbD-Assisted Squalene-based Luliconazole Entrapped Ethosomal Gel for the Skin Fungal Infection

Taqdir Singh[1] · Akash Vikal[1,3] · Preeti Patel[2] · Ghanshyam Das Gupta[1] · Shubham Thakur[1] · Balak Das Kurmi[1]

Received: 4 June 2025 / Accepted: 29 September 2025

Abstract

Fungal infections pose a significant global health challenge, especially in immunocompromised individuals. Luliconazole (LZL), a newly approved drug for topical fungal infections, faces limitations due to poor skin penetration, short skin retention time, and repeated administration. To address this, lipid nanocarrier-based ethosomal gel formulations at 1% w/w strength were developed and extensively characterized through *in vitro, ex vivo*, and *in vivo* studies, comparing them with conventional formulations. The optimized ethosomal formulations exhibited a vesicle size of 209.2 ± 8.52 nm, encapsulation efficiency of 81.51 ± 3.62%, and PDI of 0.198 ± 0.001. These ethosomes were incorporated into a gel with adhesiveness of 1.012 mJ, hardness of 0.17 N, and spreadability ranging from 7.9 to 0.52 g·cm/sec. In vitro release studies showed 84.39 ± 1.5% release for the optimized ETs-gel formulation compared to 45.58 ± 0.9% for the LZL-conventional gel. *In-vitro* activity against *Candida albicans* demonstrated superior efficacy of the prepared ethosomal formulations over the conventional gel. *Ex vivo* studies on porcine ear skin indicated enhanced penetration and skin retention time for the optimized ETs-gel compared to the conventional gel. *In-vivo* antifungal activity on albino rats confirmed the safety, non-irritant nature, and efficacy of the optimized ETs-gel in topical fungal treatment, with no systemic drug circulation observed. Histopathology studies further supported the efficacy of the optimized ETs-gel formulation. Overall, squalene-based ethosomes emerge as promising carriers for enhancing the topical delivery and localized effectiveness of Luliconazole.

Keywords anti-fungal activity · *Candida albicans* · ethosomes · luliconazole · topical formulation

Introduction

Fungal skin infections pose significant dermatological challenges globally. These infections affect a staggering number of people, with an annual incidence of over 150 million individuals. These fungal infections have wide-ranging repercussions on patients' lives, irrespective of whether they live in developed or developing countries. Fungal diseases manifest in various forms, ranging from superficial infections on the skin and mucous membranes to more severe and chronic infections within the body's internal organs. Superficial fungal infections are particularly prevalent, with an estimated global incidence of 20% to 25% [1–4]. Fungal infections, often linked to factors such as hygiene, sanitation, and access to healthcare, are a common reason for dermatological consultations. Fungi, found ubiquitously, can be classified as yeast or mold based on their morphology, with approximately 200 species pathogenic to humans among the nearly 1 million known fungal species. These infections have been associated with higher mortality rates in vulnerable groups, such as premature neonates, infants, and the elderly [5–7].

Fungal diseases are categorized into dermatophytosis, subcutaneous mycoses, systemic mycoses, and other types. Dermatophytosis, caused by fungi like *Epidermophyton, Microsporum,* and *Trichophyton,* infects skin and hair. Subcutaneous mycoses penetrate deeper skin tissue [8, 9]. They can also affect internal organs, especially in immunocompromised individuals [10]. Lipid-based nanocarriers mimic skin lipids, aiding drug delivery across biological barriers and improving efficacy. Optimizing antifungal drugs while

✉ Balak Das Kurmi
bdkurmi@gmail.com

1 Department of Pharmaceutics, ISF College of Pharmacy, GT Road, Moga-142001, Punjab, India

2 Department of Pharmaceutical Chemistry, ISF College of Pharmacy, GT Road, Moga-142001, Punjab, India

3 Sahu Onkar Saran School of Pharmacy, Faculty of Pharmacy, IFTM University, Moradabad, India

Published online: 26 November 2025

reducing resistance and toxicity remains a significant challenge in therapeutic formulation [11].

Topical, systemic, and phototherapy are the primary treatments for managing fungal infections. For moderate to severe cases (covering more than 30% of the body surface), systemic therapies are recommended as the first-line treatment along with topical formulations [12]. Additionally, topical medications are preferred as the initial choice for treating fungal infections due to their localized action, moisturizing effects, and superior skin penetration or retention time. In contrast to systemic therapy, topical treatments offer targeted action at the site of infection and are easier to apply.

Antifungal agents, particularly azoles like imidazoles and triazoles, are widely used due to their broad spectrum and effectiveness against fungal infections [13]. Clinical studies indicate that while clinical signs and symptoms often improve within 2–4 weeks, complete cure may take 12–36 weeks, depending on the infection type and site [14]. For instance, toenail infections (onychomycosis) typically require up to 12 weeks for treatment [15]. However, imidazole antifungals have drawbacks such as resistance and lengthy treatment courses lasting weeks, which can lead to poor patient adherence and disease recurrence.

Luliconazole is an azole antifungal agent which have potent activity against a variety of fungi, including those caused by *Candida Albicans species*, dermatophytes (Trichophyton and Microsporum), and certain types of yeast [16, 17]. Luliconazole, the only antifungal regulated for the short-term treatment of surface fungal infections, is classified as BCS II (low solubility and high permeability). It works by blocking ergosterol synthesis, which is required for fungal cell membranes, reducing and causing cell death. Its delivery can be challenging due to its low solubility and high lipophilicity [18]. Improving the delivery of luliconazole is essential to enhance its solubility, skin penetration, and retention, thereby optimizing therapeutic outcomes. The selection of an antifungal drug depends on factors such as the type and severity of infection, the patient's overall health, and individual considerations[19]. This study aims to develop topical gel formulations of Luliconazole using vesicular delivery systems like elastic liposomes, transferosomes, and ethosomes. These systems promise improved ski.

n permeation and targeted treatment of fungal infections, reducing systemic absorption and adverse effects. Their nanometric size, high drug loading, and enhanced solubility offer advantages, complemented by gelling agents to ensure compatibility with cream and gel bases for elegant and stable formulations [20].

Sebum, secreted from sebaceous ducts, consists primarily of squalene (12–15%) along with wax esters and glycerides. Therefore, incorporating squalene into topical formulations could potentially restore the lipid content of sebum. The major mechanism involved in drug transfer from the external environment to the lipid or sebum layers within the skin is partitioning. This process can be facilitated by formulating lipid carriers for the intended drugs [21]. Lipid carriers readily assimilate into the skin's lipid environment, forming a drug depot within the skin. Ethosomes are lipid vesicular carriers that contain a relatively high amount of ethanol for improved medication penetration through the skin. They mostly consist of water, ethanol, and phospholipids. The high ethanol content, which fundamentally sets ethosomes apart from other vesicular carriers, works to increase epidermal penetration and release the drug particles [22, 23]. Ethosomes are particularly suited for drugs classified under BCS classes II and IV due to their ability to enhance solubility. They improve topical drug efficacy by effectively merging with sebum in follicles. Compared to liposomes or niosomes, ethosomes offer better control over drug release and higher drug entrapment within lipid environments, thanks to the arrangement of solid and liquid lipids, which provides more surface area and space for dissolved drugs [24, 25]. Consequently, ethosomes exhibit higher drug loading capacity. To enhance the partitioning of lipid carriers into the stratum corneum of the skin, it is essential to maintain a hydrated environment at the targeted skin site [22, 26]. The novelty of this research we are using a shark liver oil, which is also known as squalene with the help to this oil formulate a squalene-based nanocarrier. The nanocarrier is increasing the penetration of the drug, and squalene is increasing the dermal retention time, because squalene is secreted by sebum, which is present in skin dermis layer so this formulated squalene-based nanocarrier is helpful to retain the drug on the dermis layer and provide the moisture content on the skin[21]. Overall the squalene based nanoocarrier is overcome the limitation of luliconazole gel.

The present study, we hypothesized that the squalene-based luliconazole-loaded ethosomal gel would enhance penetration, increase skin moisture content, and increase dermis layer retention time. Overall, the ethosomal gel may give better antifungal activity. In this study, we aimed to develop gel formulations incorporating vesicular systems to improve the topical delivery of Luliconazole, maintaining a drug content of 1% w/w consistent with commercial strengths. These formulations were evaluated against conventional marketed products through *in vitro* drug release studies, *in vitro* antifungal activity assessments, and *ex vivo* permeation and deposition potential using porcine ear membranes. Additionally, the optimized formulation's *in vivo* antifungal efficacy was tested, alongside histopathological analysis of treated rat skin.

Materials and Methods

Materials

Luliconazole was obtained as a gift sample from Zydus Cadila Pvt. Ltd.Carbomer (Carbopol 974 A NF), methyl

alcohol, and chloroform were purchased from Himedia Pvt. Ltd., India. We bought squalene, tween 80, from LOBA Chemicals Pvt. Ltd. in India. Sigma-Aldrich Pvt. Ltd., India, supplied the phospholipid.

QbD Approach

Establishing CQAs and Defining QTPP

The first step in Quality by Design (QbD) driven development involves establishing the Quality Target Product Profile (QTPP), delineating the expected quality characteristics of the targeted therapeutic product. Here, the aim is to develop a stable ethosomal formulation that can efficiently deliver a substantial dose of luliconazole, thereby enhancing skin penetration, skin retention and increasing localized effect. These objectives encapsulate the desired outcomes regarding the product's effectiveness. Therefore, the QTPP shows a foundation for developing a product that maintains quality, safety, and efficacy. It includes important elements like dosage form, route of administration, stability, and particular product characteristics like skin permeability. The goal of formulation development is to consider these factors to deliver a product that conforms to quality standards and effectively fulfills its intended therapeutic goals.

Optimization of Luliconazole-loaded Ethosomes Through DoE (Box-Behnken Design)

A Box-Behnken design (BBD) with three factors and three levels was used to optimize critical material attributes (CMAs) affecting key quality indicators. The factors—phospholipid quantity (X1), ethanol concentration (X2), and squalene amount (X3)—were evaluated at actual and coded levels $(-1, 0, +1)$. Critical quality attributes (CQAs), including vesicle size (Y1), entrapment efficiency (Y2), and polydispersity index (Y3), were assessed. Seventeen batches, including five center points per block, were prepared in triplicate for reliability, with other variables held constant to minimize confounding factors.

ANOVA

Multiple linear regression analysis (MLRA) was performed using Design Expert software to assess the impact of independent variables on the response variables. Second-order polynomial models were developed to capture factor-response relationships, validated through analysis of variance (ANOVA). Software equations were analyzed to assess the influence of each critical material attribute (CMA). Visual tools, such as 3D response surface plots, 2D perturbation curves, and contour plots, were used to gain insights into the effects of the variables. Goals were set based on the desired results, and validation batches were created using the software's desirability strategy to find optimal CMA concentrations for target critical quality attributes (CQAs). Actual results from the optimized formulation were compared with software predictions to assess model accuracy and reliability.

Pre-formulation Studies

Pre-formulation studies are a series of experiments and tests conducted on the drug to determine its physical and chemical properties before formulation development. This study provided critical information for formulators to design and develop safe, stable, and effective drug products.

Physical Appearance

Physical appearance of a drug, like color and description, was analyzed by visual observation [27].

Melting Point Determination

To determine the melting point of the drug, it was first loaded into an open-ended capillary tube. Subsequently, a Perfit Digital Melting Point Apparatus was utilized to precisely measure the temperature at which the drug began to melt. This method ensures accurate determination of the drug's melting point by providing a controlled environment and reliable temperature measurement capabilities [27].

FT-IR

FT-IR spectroscopy is a valuable method for analyzing and characterizing drugs. The FTIR spectrum of a drug can provide valuable information about the structure and composition of the drug. This information can be used to identify the drug, determine its purity, and study its chemical properties. A KBr pellet was prepared by grinding KBr crystals into a fine powder. A small amount of the drug was added to the KBr powder and mixed well. The KBr/drug mixture was pressed into a pellet using a hydraulic press. The KBr/drug pellet was loaded into the FTIR spectrometer. The FTIR spectrum of the drug was collected. The FTIR spectrum was analyzed to identify the functional groups present in the drug [27, 28].

Compatibility Studies of Drug and Excipients by FTIR Spectroscopy

FTIR spectra were obtained for Soya lecithin and a physical mixture of Soya lecithin with Luliconazole to assess

compatibility. The KBr disc method involved grinding 1 mg of each substance into a fine powder, compressing them into discs, and analyzing the spectra for any new peaks. The absence of additional peaks in the physical mixture confirmed compatibility between the excipient and the drug [28].

Partition Coefficient

The shaking flask method was used to determine luliconazole's partition coefficient. The partition coefficient of luliconazole was determined using a 10-mL solution containing a 1:1 mixture of n-octanol and acetate buffer (5.5). To ensure equilibrium, 10 mg of luliconazole was added, and the process was repeated three times. The mixtures were mixed in separating funnels for 24 h. The organic and aqueous phases were separated once equilibrium had been achieved. The concentration of luliconazole in both phases was determined with a UV spectrophotometer (UV-1800, Shimadzu, India) at a wavelength of 295 nm. The partition coefficient was then calculated using the appropriate equation[27`].

DSC of Luliconazole

DSC analysis was conducted using the DSC6000. Each sample, weighing 10 mg, was placed in an aluminum pan and subjected to a scanning rate of 10 °C/min. The temperature range of the analysis is from 0 to 800 °C under an inert atmosphere of nitrogen [29].

Determination of λmax for Luliconazole in Methanol

The accurately weighed 10 mg of Luliconazole was initially dissolved in methanol to prepare a stock solution of 1000 µg/ml. From this, 1 ml was further diluted to 10 ml with methanol to obtain a concentration of 100 µg/ml. A 0.1 ml aliquot of this solution was then diluted to 10 ml with methanol to achieve a final concentration of 10 µg/ml. The absorbance spectrum of the 10 µg/ml solution was scanned across wavelengths from 200 to 400 nm to identify the wavelength of maximum absorbance [30].

Calibration Curve of Luliconazole

In Methanol: Acetate Buffer (5.5) Luliconazole 10 mg was weighed and dissolved in 10 ml of methanol by gentle shaking, resulting in a concentration of 1000 µg/ml. From this solution, 1 ml was transferred and diluted to 10 ml using acetate buffer (5.5), resulting in a stock solution with a concentration of 100 µg/ml. Aliquots of 2, 4, 6, 8, 10, 12 µg/mL were prepared from this stock solution and diluted to 10 mL with acetate buffer (5.5), resulting in dilutions ranging from 10 to 100 µg/mL. These prepared dilutions were analyzed using UV-spectroscopy to measure peak areas at 295 nm, and a standard curve was constructed plotting peak areas against the drug concentration [29].

In Methanol: PBS (7.4) Luliconazole 10 mg was weighed and dissolved in 10 ml of methanol by gentle shaking, resulting in a concentration of 1000 µg/ml. From this solution, 1 ml was transferred and diluted to 10 ml using a pH 7.4 buffer, resulting in a stock solution with a concentration of 100 µg/ml. From the stock solution, concentrations of 2, 4, 6, 8, 10, 12 µg/ml in pH 7.4 buffer were prepared. The absorbance of these diluted solutions was measured at 295 nm, and the correlation coefficient was subsequently identified [31].

Method

Preparation of Ethosome via the thin Film Hydration Method

To prepare deformable ethosomes, the drug was initially dissolved in 3 mL of methanol, while the lipid phase, containing soya lecithin both was dissolved in chloroform. The solvent was evaporated under reduced pressure in a rotary evaporator at 50 °C until a thin film formed on the flask wall. Evaporation continued for 2 h after the film appeared dry to ensure complete solvent removal. Next, the film was hydrated using a solution of squalene in a mixture of ethanol and water (3:7 ratio). The hydration process involved heating in a water bath at 50 °C for 10 min, followed by vortexing for 2 min. The resulting dispersion was then sealed hermetically, protected from light, and stored at 4 °C[32].

Characterization of LZL-Ethosomes

Evaluation of Particle Size, Zeta Potential, and Polydispersity Index Particle size analysis of LZL was conducted using Dynamic Light Scattering (DLS) with a Zetasizer (ZS nano 3600, Malvern Instruments, UK). Before analysis, the LZL samples were diluted tenfold with Milli-Q water. Measurements for particle size, polydispersity index (PDI), and zeta potential were performed in triplicate at a controlled temperature of 25 °C. DLS provides valuable insights into the size distribution and surface charge of nanoparticles by analyzing fluctuations in light scattering intensity caused by Brownian motion. This method ensures accurate characterization of LZL properties under standardized conditions [27].

Morphological Assessment Using TEM Morphological analysis aimed to define sample characteristics and shape. A portion was placed on a carbon-coated copper grid, stained with phosphotungstic acid for visibility. After air-drying, examination via transmission electron microscope (TEM) captured photos documenting the colloidal system morphology [33].

Determination of Entrapment Efficiency(%EE) and Loading Capacity of Ethosomes Containing Luliconazole (LZL) To determine the %EE of ethosomes, a widely accepted indirect method was utilized. Samples of LZL-ETs were centrifuged using a cooling centrifuge (Remi: C-24 BL, India), separating the supernatant containing free LZL from the entrapped drug. Afterwards, LZL content was determined by diluting the samples with methanol and performing spectrophotometric analysis at 295 nm using a validated method, which allowed for the calculation of ethosome entrapment efficiency and loading capacity using a defined mathematical formula [34, 35].

$$\%\ \text{Entrapment Efficency} = \frac{\text{Total amount of LZL dded} - \text{Amount of LZL unentrapped}}{\text{Total amount of LZL added}} \times 100$$

$$\%\ \text{Loading Efficiency} = \frac{\text{Total amount of LZL added} - \text{Amount of LZL unentrapped}}{\text{Total amount of formulation}} \times 100$$

Development of Ethosomes-embedded Carbomer-based gel Formulation The Ethosomal formulation was converted to gel using Carbopol 934 as a gelling agent. Gel was prepared by dissolving 500 mg of Carbopol 934 into 50 ml of distilled water to form 1% (w/w) gel and kept aside for 24 h. After swelling and hydration, the gel base was prepared. Then take 1 g of Carbopol gel from the prepared base. Then, the optimized Luliconazole-loaded Ethosomal solution was added to the gel with constant stirring for 20 min. Then, homogeneity was ensured by constant stirring at 1000 rpm for an h. Add 0.2 ml of triethanolamine, which raised the pH and promoted gel formation, the liquid was given the appropriate consistency and gelling qualities. The pH of the gel was maintained in the range of 6–7 [36].

Characterization of Formulated Ethosomal Gel

- Texture Analysis

  A formulation of ETs gel with about 1% w/w concentration was prepared and characterized using a CT3 texture analyzer (Brookfield Engineering Lab, Inc., USA), The prepared gel was tested for mechanical criteria such as hardness, cohesiveness, and adhesiveness. An analytical probe with a diameter of 3.5 cm for a single cycle at a specified rate of 0.5 mm/s, with a 5 kg load cell for the analysis, was used [33].

- Determination of pH

  To determine the pH of LZL-ETs-gel, a specific procedure was followed. Firstly, 1 gram of each formulation was diluted in 50 mL of distilled water and thoroughly mixed for 30 minutes using a magnetic stirrer at room temperature. Subsequently, the pH of the diluted formulations was measured using a calibrated pH meter (Mettler Toledo FE20-I-Kit). To ensure accuracy and reliability, all measurements were performed in triplicate. This standardized approach and triplicate measurements ensured precise and consistent pH values for both formulations.

- Spreadability using the Plate Method

  The spreadability of the hydrogel formulations was evaluated using the plate method. A small amount of both LZL-ETs-gel was placed between two acrylic plates and pressed together for 5 minutes. As the gel spread out, forming circles, the initial and final diameters of these circles were measured. Analyzing the increase in diameter allowed for assessing the spreadability of the gel. This evaluation offered valuable insights into the physical properties and performance of the hydrogel formulations[34].

***In-vitro* Anti-Fungal Activity** The *in-vitro* anti-fungal activity of Free drug (LZL-solution), LZL-ETs-gel and LZL-conventional gel formulations against *C. albicans* was assessed using the agar plate method. *In vitro* antifungal research, the free drug solution serves as a positive control for evaluating the maximum antifungal activity of the active agent. It provides direct comparison with formulations to evaluate the effectiveness of drug release, the effect of excipients, and the overall performance of the formulation. Its inclusion represents a standard scientific approach to ensure the reliability, reproducibility, and validity of experimental results in antifungal efficacy studies. *Candida albicans* cultures was that they were activated again and plated on Petri dishes containing nutrient agar media. Holes were created in the agar surface using a 5 mm diameter borer. The nutrient agar surface was then inoculated with 100 µL of C. albicans suspension. Next, wells were prepared and filled with LZL-solution, LZL-ETs-gel, and LZL-conventional gel formulations at identical concentrations. Following incubation at 37 °C

for 48 h to enhance the growth and interaction between the formulations and *C. albicans*. The plates were examined for zones of inhibition to assess the formulations' effectiveness against the fungus. The diameters of these zones were measured and recorded to quantify the antifungal activity of the formulations [37].

***In-vitro* Drug Release** *In-vitro* drug release studies using a 1.2 kD molecular weight cutoff dialysis membrane evaluated LZL drug solution, LZL conventional gel, and LZL-ETs-GEL formulations. Each formulation containing 10 mg LZL equivalent was placed in the membrane and submerged in 50 mL acetate buffer (pH 5.5) and methanol (70:30 v/v) at 37 ± 0.5 °C with continuous stirring. Because drug solubility is main concern the use of 30% methanol in 70% acetate buffer (pH 5.5) was essential due to Luliconazole's poor aqueous solubility and high lipophilicity (BCS Class II) it means a lipophilic nature. This solvent system enabled complete solubilization and accurate UV spectroscopic quantification, as lower methanol levels (e.g., 20%) led to poor solubility, non-linear calibration curves, and inconsistent absorbance. To ensure analytical consistency and eliminate matrix-related variability, the same medium was used for both the calibration curve and in vitro release studies. This approach ensures that the UV absorbance measurements in IVR testing are directly comparable and accurately interpretable using the established calibration curve. Samples were collected at 0, 2, 4, 6, 8, 10, and 12 h, or maintained in the sink condition, and spectrophotometric analysis was performed.

Skin Permeation Study Skin permeation experiments using porcine ear skin from a local slaughter involved LZL free drug solution, LZL conventional gel, and LZL-ETs-GEL formulations. After shaving to remove hair and washing with physiological saline, skin fat was carefully cut for uniformity. Franz diffusion cells with a methanol and pH 7.4 buffer solution (3:7 v/v) at 37 ± 0.5 °C and 100 rpm facilitated sampling over time for UV-spectrophotometric analysis (295 nm) to monitor LZL permeation and release. After removing skin membranes post-Franz diffusion cell experiment, residual formulation on the epidermis was cleansed with 50% methanol, followed by fragmentation and treatment with 0.05% trypsin solution for 24 h at 37 °C and 100 rpm agitation [38]. Samples are filtered to determine LZL content using UV spectrophotometry (295 nm) for assessing LZL deposition within the skin membrane [33, 39].

In-vivo Anti-fungal Activity

Anti-fungal Activity A total of 24 albino rats were developed into the following four groups and each group have six rats: Normal control(A), Control (infected and untreated) (B), Optimized ethosomal gel treated(C), conventional gel treated(D). (ISFCP/IAEC/CCSEA/Meeting No: 05/2024/Protocol No. 41) Prior to the research, the rats underwent ten days of intraperitoneal injection of dexamethasone at a dose of 5 mg/kg/day to suppress their immune systems. Following this stage of immunological suppression, dermal infection began. Before the rats were inoculated, a 3 cm × 3 cm section of their dorsal region was shaved at least 24 h beforehand, and skin abrasions were produced. After administering anesthesia, 1 ml of culture containing 5 × 104 cells/ml was inoculated into the animals. After 7 days, the animals showed white fungal scales on their skin similar to Candida culture. Skin scales from each group expect normal control were collected on sterile paper and inoculated onto Yeast Malt Agar petri plates. These plates were incubated at 28 °C for 24 h in a Bio-Oxygen Demand (BOD) incubator. Colony Forming Units (CFUs) were counted on the plates from all three groups to assess fungal growth. After infection, topical treatments were applied daily for 7 days, except for the normal control and untreated control group. Groups C and D received optimized LZL-ETs gel and LZL-conventional gel. Physical changes on the skin were documented with photographs. After treatment, CFUs were counted again to compare fungal growth to initial levels.

Histopathology Study In the histopathology study, two animals per group were euthanized under anesthesia via spinal dislocation. After the treatment period, skin samples were excised, fixed in 10% formalin, and processed for paraffin embedding at a histological facility. Sections were sliced from the paraffin blocks, stained with haematoxylin and eosin (H&E), and mounted on glass slides for subsequent examination under a high-power light microscope. Images were then captured for detailed histopathological analysis [33].

Skin Irritation Study To conduct the skin irritation test, a shaved 1 cm2 area of the rat's skin was equally covered with a small amount of the formulation. A uniform grading system was employed to determine the degree of irritation, with scores ranging from 0 (no erythema) to 4 (fiery redness combined with swelling), facilitating consistent evaluation of the degree of redness.

Results and Discussion

Quality by Design Approach

Identifying CQAs and Defining QTPP

The Quality Target Product Profile (QTPP) and associated goals for developing ethosomal formulation with

luliconazole is compatible with ICH guidelines and preliminary formulation assessments. The objective is to maximize pharmacodynamic characteristics and improve penetration into the basal layer of the epidermis by selecting Critical Quality Attributes (CQAs) based on the Quality Target Product Profile (QTPP). Vesicular size, entrapment efficiency, and polydispersity index of luliconazole ethosomes were identified as crucial for enhancing drug permeation and retention in the dermal layer. These selections were validated with solid rationale from literature, previous research, and established knowledge. Optimal vesicle size and Polydispersity Index (PDI) are pivotal, balancing skin penetration benefits with systemic absorption risks. Maximized entrapment efficiency is essential for optimal therapeutic outcomes, emphasizing ethosomal gel for enhanced skin penetration and retention, aiming for sustained release and avoiding systemic effects. The formulation targets a vesicle size of 100–300 nm, high entrapment efficiency, and minimal PDI to ensure stable and effective therapeutic outcomes.

Design of Experiments (DoE)

The Box-Behnken design is used, the selected independent factors affecting the final responses were simultaneously optimized after the Quality Target Product Profile (QTTP) and Critical Quality Attributes (CQA) were confirmed and (Table I & II) provides a brief overview of all the experimental procedures. The seventeen experimental runs were devised using the Box-Behnken Design, the result of particle size, entrapment efficiency and PDI, subsequent observations were thoroughly recorded which are show in (Table III). The Analysis of Variance (ANOVA) evaluates the significance of the mathematical model by assessing variations, incorporating an adjusted R2 value and a lack of fit test, both exceeding the 0.9 threshold. The collected observations indicated a p-value < 0.0001 for X1, X2, and X3, highlighting the significance of these variables in the model. This suggests potential for further optimization research. Overall, the study demonstrates a strong correlation and compatibility with the statistical analysis [35, 40]. In all polynomial equations and perturbation plots, software-generated coded variables A, B, and C correspond to the actual independent variables X1 (Phospholipids), X2 (Ethanol), and X3 (Squalene), respectively. The use of coded terms ensures simplified interpretation of statistical interactions.

Polynomial Equation

Effect of Critical Material Attributes on Vesical Size (Y1) The response showed by software that the effect of variable on particle size is following quadric equation and the equation was found to be

$$\begin{aligned} \text{VS (Y1)} &= 194.2 + 99.65A + -14.1625B + -23.6875C \\ &+ -20.6\,AB + -6.05\,AC + -3.925\,BC \\ &+ 83.8625\,A^2 + 6.1375\,B^2 + 11.3875\,C^2 \end{aligned}$$

The impact of independent variables X1, X2, and X3 on Y1 was assessed using permutation, polynomial, and contour analyses. Positive signs indicated synergism, while negative signs indicated antagonism in their effects on the response. X1 and X2 predominantly reduced Y1 positively, favoring excipient compatibility but increasing risk to the response. Combined interactions (X1X2, X2X3, X1X3) led to temporary decreases in particle size, ensuring formulation stability. Perturbation analysis (Fig. 2) showed no significant inherent interactions among variables. The 3D contour plot and blend dependency graph (Fig. 1) illustrated the quadratic equation's influence. Increasing X1 and X3 antagonistically increased size, whereas incorporating X2 with X1 and X3 produced nanosized ethosomes (160.9–420.3 nm).

Table I Box-Behnken design using both coded and actual values, distinguishing between independent and dependent variables is crucial

Factor	Name	Type	Low Actual	High Actual	Low Coded	High Coded	Mean
X1	Phospholipids (mg)	Numeric	200	400	−1	+1	300
X2	Concentration of ethanol (ml)	Numeric	20	60	−1	+1	40
X3	Squalene (µL)	Numeric	120	160	−1	+1	140

Table II Dependent variable Y1, Y2, Y3 minimum and maximum value

Response	Name	Unit	Obs	Analysis	Minimum	Maximum
Y1	Vesical size	nm	17	Polynomial	160	424
Y2	Entrapment efficiency	%	17	Polynomial	34	89.5
Y3	Polydispersity index	–	17	Polynomial	0.199	0.374

Table III The experimental 17 runs were devised using the Box-Behnken Design, the result of particle size, entrapment efficiency and PDI observations

Runs	Phospholipid mg (X1)	Concentration of ethanol % (X2)	Squalene µL (X3)	Vesicular Size (nm) (Y1)	% EE (Y2)	PDI (Y3)
1	0	0	0	200.5	70.1	0.216
2	0	0	0	195.5	65.3	0.21
3	0	0	0	163.4	61.9	0.23
4	0	0	0	200.9	64.2	0.199
5	0	0	0	210.7	66.7	0.194
6	0	1	1	160.9	34.8	0.371
7	0	−1	1	210.4	65.6	0.374
8	0	1	−1	220.9	50.5	0.356
9	0	−1	−1	254.7	86.1	0.223
10	1	0	1	365.6	52.6	0.362
11	−1	0	1	170.7	42.5	0.334
12	1	0	−1	424.3	82.8	0.293
13	−1	0	−1	201.2	63.4	0.266
14	1	1	0	351.9	44.2	0.294
15	−1	1	0	201.5	38.4	0.316
16	1	−1	0	408.1	89.5	0.326
17	−1	−1	0	175.3	61.7	0.229

Effect of CMAs on the Entrapment Efficiency (Y2) The Design of Experiments (DOE) approaches were also used to evaluate the effects of particular variables on Y2. The polynomial equation shows the positive outcome of statistical optimization, showing that the factors' combined synergistic effect produced a desired entrapment efficiency result. The entrapment efficiency varied between 34.4% and 89.5%, indicating a noteworthy 20-fold increase in Y1 via the combined interaction factors. Perturbation analysis, depicted in Fig. 2 and 3D plot, indicated no need for log or power transformations, affirming the suitability of proposed variables for the study. Analysis highlighted X1 and X3 significantly enhance luliconazole encapsulation efficiency, while X2's negative linear coefficient shows ethanol diminishes entrapment, consistent with prior research. X2 exhibits a quadratic effect within 30–50 ml, influenced by X1 and X3, achieving 89.5% efficiency. Stable interaction among X1, X2, and X3 defines an effective design space for optimizing entrapment efficiency.

$$\begin{aligned}\text{EE (Y2)} &= 65.64 + 7.7625\,\text{A} + -16.75\,\text{B} + -10.9125\,\text{C} \\ &+ -5.25\,\text{AB} + -2.325\,\text{AC} + 1.2\,\text{BC} \\ &+ -3.1825\,\text{A}^2 + -4.2575\,\text{B}^2 + -2.1325\,\text{C}^2\end{aligned}$$

Effect of CMAs on the PDI of Ethosomes (Y3) The polydispersity index (PDI) serves as a crucial indicator of vesicle stability in ethosomes, reflecting the formulation's size homogeneity and dispersion-mediated stability. The influence of X2 and X3, particularly at a 40% concentration, acts as a co-amphiphilic, reducing interfacial tension and promoting stable compatibility, thereby favoring PDI reduction (Fig. 1) Additionally, positive outcomes from combined interaction terms align with vesicle size analysis above 126.2 µL have a neutral effect on X1, while increasing X2 and X3 concentrations contribute to stable responses. Thus, the analysis suggests an independent relationship between X1 and X3, with X1, X2, and X3 identified as potential variables for optimal response effects.

Analysis of Variances The analysis of variance (ANOVA) in confirms the significance of the mathematical model. Key statistical tests, including lack of fit and an adjusted R2 value exceeding 0.9, underscore the model's robustness. The p-values for X1, X2, and X3 (<0.0001) indicate significant model terms relative to these variables, validating their relevance for optimization studies. Overall, the fit statistics are strongly aligned with the study's objectives.

Pre-formulation Studies

Physical Appearance

The luliconazole was visually inspected and found to be white crystalline powder, odorless as illustrated in the Indian pharmacopeia monograph.

Melting Point

The melting point of Luliconazole was determined to be 153–160 °C using a validated method, ensuring

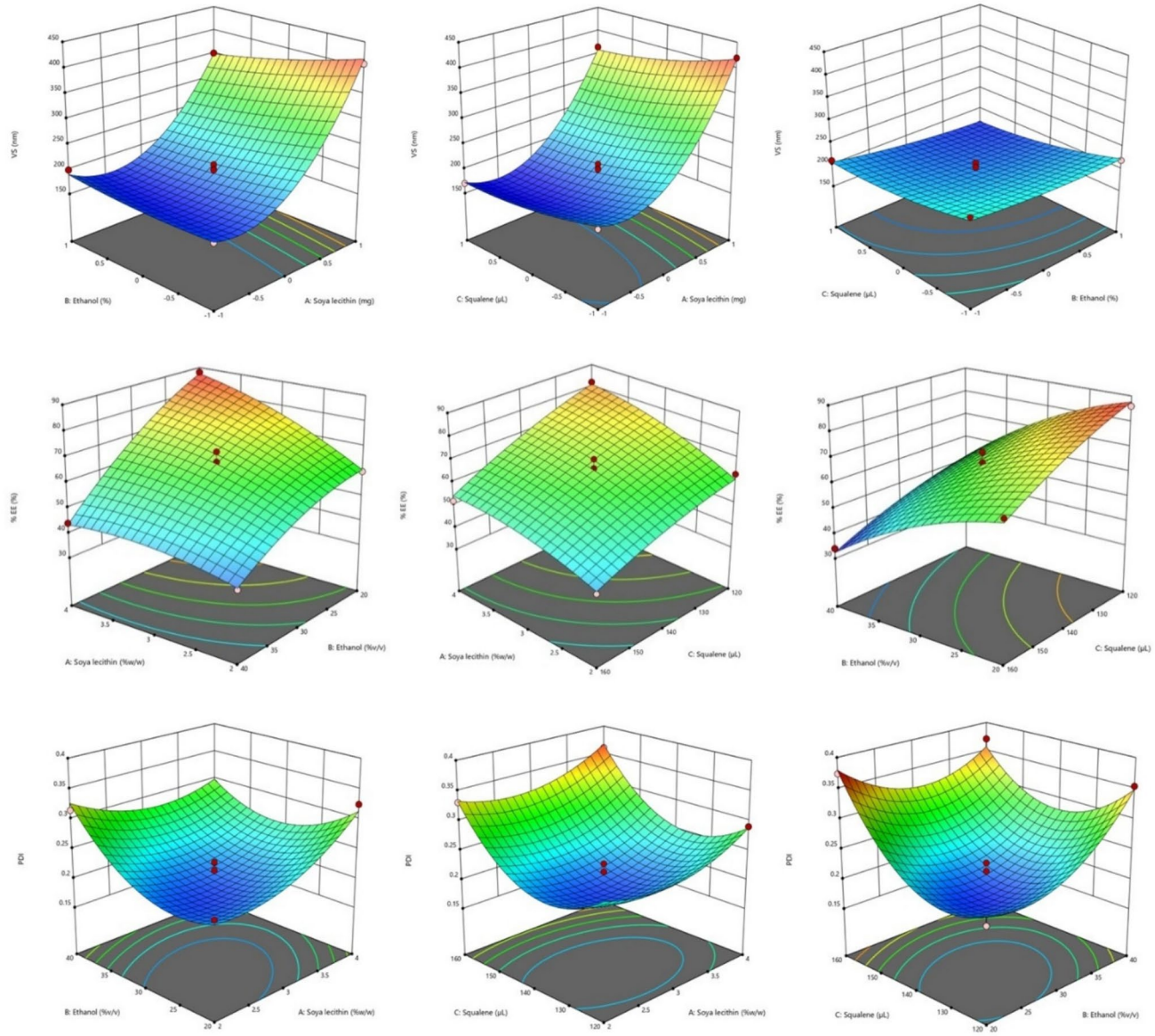

Fig. 1 Three-dimensional (3D) plot shows the effect of independent variable on dependent variable

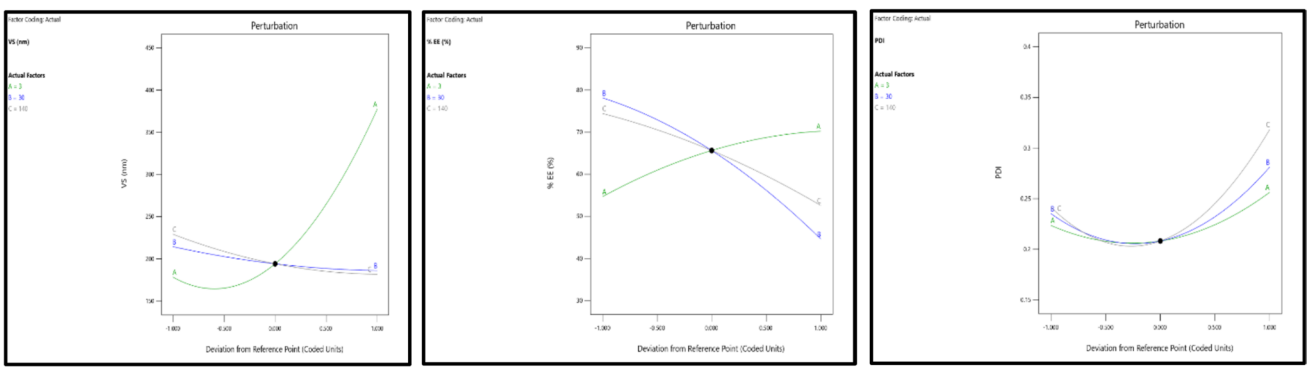

Fig. 2 Perturbation analysis of effect of the independent variable on dependent variable

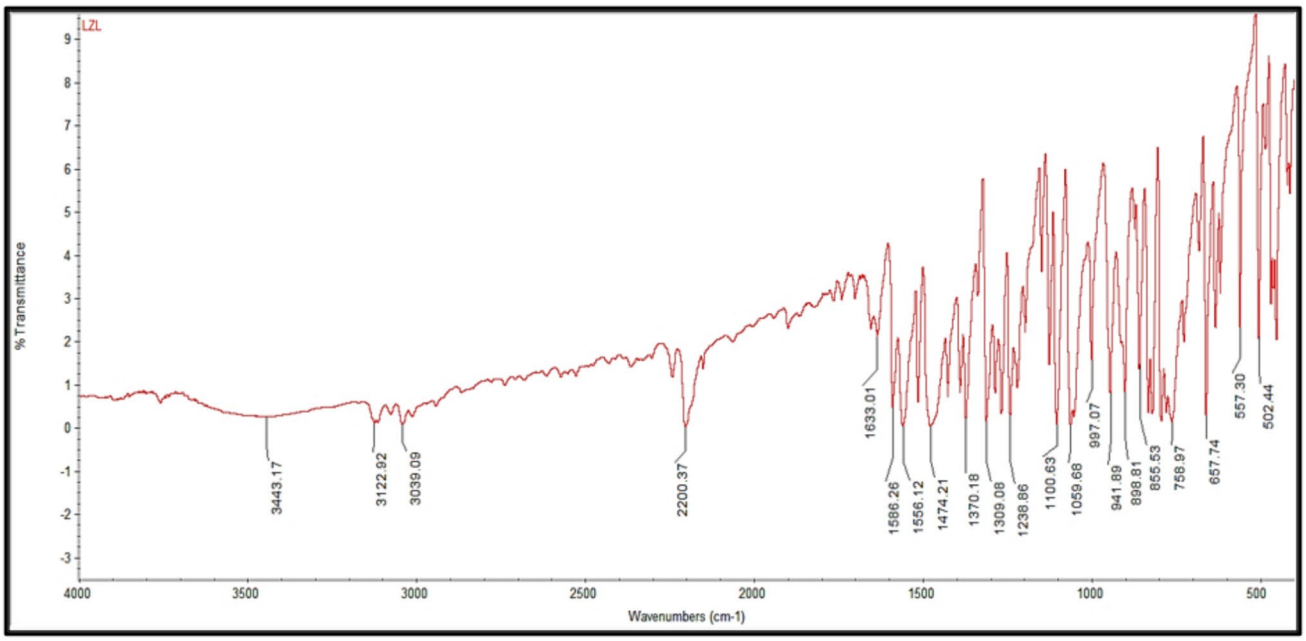

Fig. 3 FTIR spectra of Luliconazole

accuracy[41]. This property is crucial for assessing the compound's purity, as a pure sample displays a sharp melting point. Impurities can broaden this range. Luliconazole's melting point also impacts its formulation into creams and ointments; it must be lower than the formulation's melting point for uniform distribution[42]. Factors like purity, impurities, and storage conditions influence luliconazole melting point. Consistency with the literature value suggests purity.

Partition Coefficient

The partition coefficient (log10 P) of luliconazole was determined to be 3.803 ± 0.001 indicating its lipophilic nature[16].

Fourier Transform Infrared (FTIR) Spectroscopy

FTIR Spectrum of LZL was obtained by scanning the drug in the range of 4000 to 400 cm^{-1}. Major peaks observed were as 657 $cm^{-1}$and 1059 cm^{-1} (Aromatic C–Cl Stretch), 1586 (C = C aromatic stretch), C-N (1238 cm^{-1}, 1309 cm^{-1}), C = N (1633 cm^{-1}), C≡N (2200 cm^{-1}), C–C (3039 cm^{-1}) whose presence resembled the structure of LZL[27].Observed FTIR spectra and standard value were as depicted in Fig. 3**.** The observed value was within the range or very close to the characteristic peaks of standard value confirming drug as LZL.

Compatibility Studies of Drug and Excipients by FTIR Spectroscopy

The lack of significant changes in the FTIR spectra after physical mixing the drug and excipients indicates no chemical incompatibility. This assures the accurate mixing without compromising Luliconazole's stability. The presence of characteristic functional groups in the excipients suggests potential interactions, yet further studies are necessary for confirmation. The stacked spectra of Luliconazole and soy lecithin in Fig. 4 demonstrate no notable changes post-mixing, reinforcing the absence of chemical incompatibility and ensuring safe combination without affecting Luliconazole's stability.

Determination of Absorption Maxima Using UV–Visible Spectroscopy

The absorption maxima of λ_{max} of LZL in methanol were found to be 295 nm. The absorption maximum of luliconazole was determined according to standard protocol at 295 nm (λmax) across concentrations ranging from 2–10 µg/ml. The regression equation obtained was 0.0739x—0.0063,

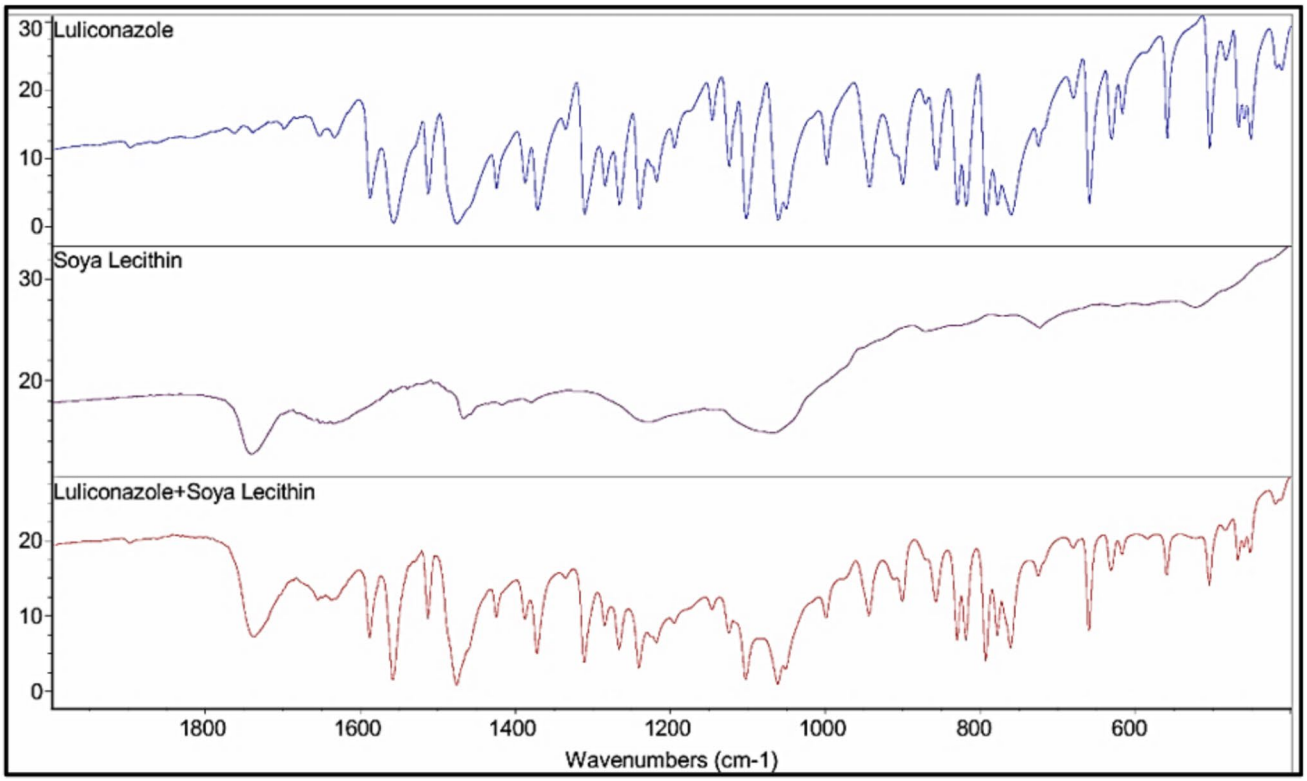

Fig. 4 FTIR-Based Drug-Excipient Compatibility Analysis

with a coefficient of determination (R^2) of 0.9954. This study aimed to validate methods for both qualitative and quantitative analysis of luliconazole absorption [41].

Calibration Curve in Methanol: Acetate Buffer (5.5) The calibration curve of LZL was prepared using methanol: acetate buffer (5.5). The result shows linearity, and the R2 value is 0.9979 [31].

Calibration Curve in Methanol: PBS Buffer (7.4) The calibration curve of LZL was prepared using methanol: PBS buffer 7.4. The result shows linearity, and the R2 value is 0.9954. This confirms the reliability of the selected analytical method, likely UV spectrophotometry, for analysing luliconazole encapsulated in the lipid-based nano-formulation. The high coefficient of determination (R2) guarantees precise determination of drug concentration through absorbance measurements, enabling accurate assessment of drug loading and encapsulation efficiency in the nano-formulation [43].

DSC

The DSC thermogram of the drug is shown in Fig. 5**.** The drug endothermic peak is 160.84° C, which is consistent with its reported value. The DSC endothermic peak indicates that the drug is crystalline [29].

Size and Polydispersity Index, and Morphological Evaluation

The ethosomes had an average vesicular size of 209 ± 9.82 nm (Fig. 6a). The polydispersity index (PDI) was 0.198 ± 0.001, indicating a uniform size distribution of the nanoparticles. Ethosomes with these characteristics enable easy penetration through the stratum corneum, enhancing their effectiveness. Figure 6, (a) [35]. Low PDI values highlight the colloidal carriers' homogeneity and stability, ideal for effective topical drug delivery to the skin [44]. The morphological evaluation, conducted through TEM images, revealed that the ethosomes exhibited a spherical shape and 200 nm size is observed [45, 46]. Figure 6(b): Size scale which is shows TEM image in red colour.

Entrapment Efficiency and Drug Loading

Entrapment efficiency of the optimized batch was 81.5 ± 0.56%, and drug loading was found to be 28.5 ± 1.1%, respectively. The high entrapment efficiency

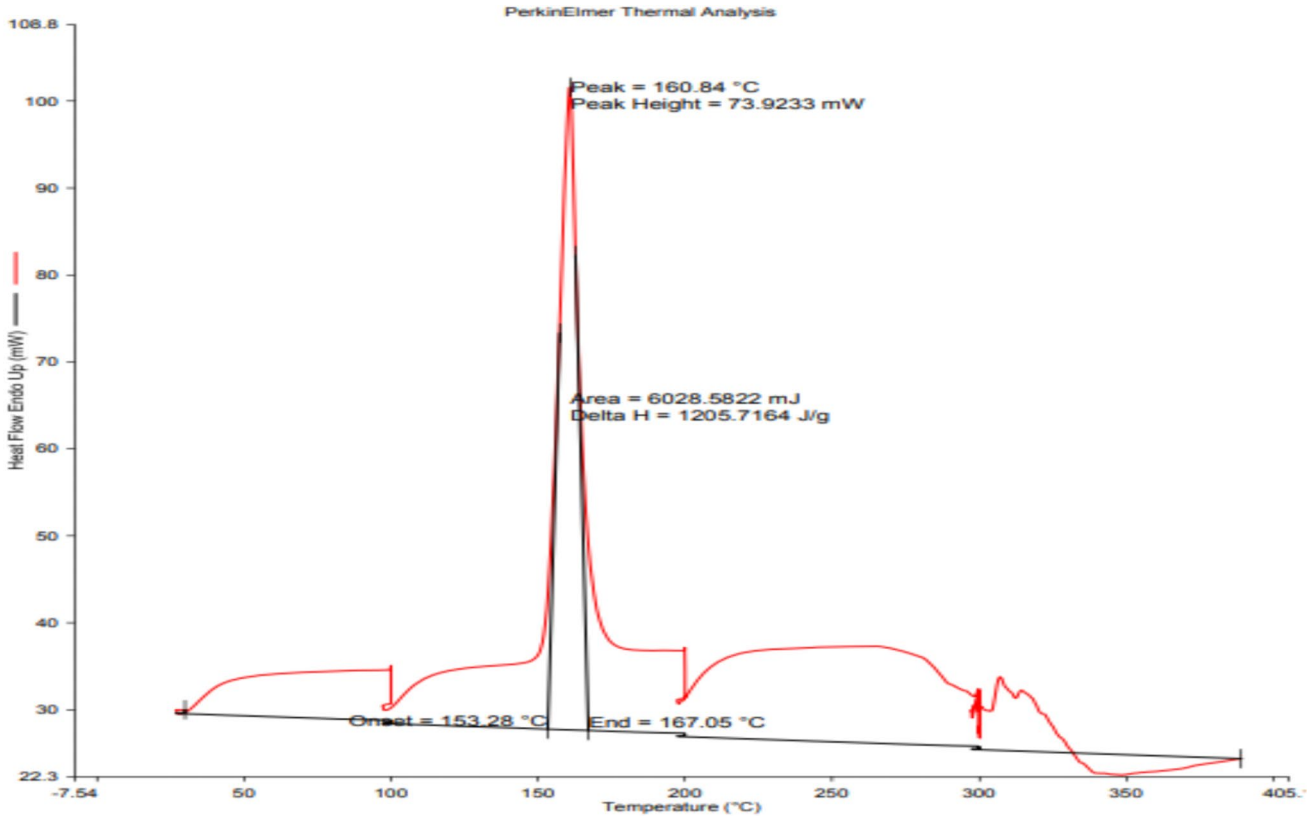

Fig. 5 DSC thermogram of luliconazole

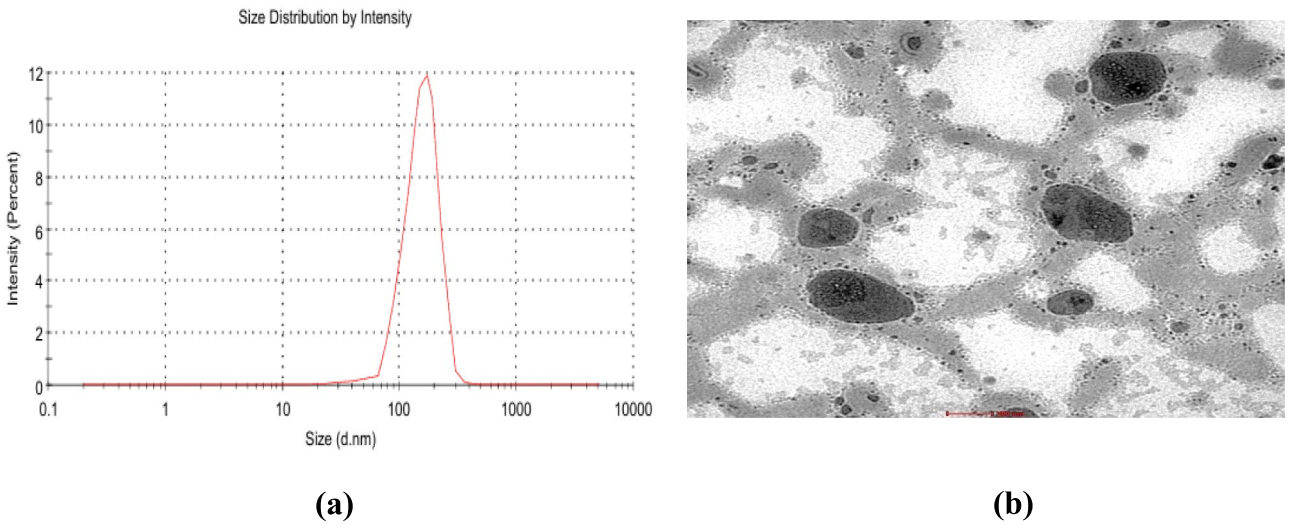

Fig. 6 **a** Intensity distribution graph of optimized formulation, **b** morphological evaluation of optimized TEM

of ETs makes them a promising drug delivery system for a variety of applications. The results indicate that ethosomes are faster at absorbing and transferring the lipophilic substance LZL. The capacity to promote topical drug distribution proves extremely valuable, especially when it comes to treating fungal diseases [41].

Characterization of Gel

Texture Analysis of Gel: Evaluation of pH, Adhesiveness, Stringiness

The gel formulation exhibited a pH of 6.74 ± 0.3. Adhesiveness measured at 1.012 mJ, stringiness length at 0.213 cm, and hardness at 0.17 N. Carbopol 934 and HPMC serve as thickening and gelling agents. Carbopol 934 formed a stronger gel compared to HPMC. This implies that Carbopol 934 gels are less adhesive, have shorter stringiness lengths, and are harder than HPMC gels. Lower concentrations of HPMC maintained gel stringiness. Upon application to the skin, the gel exhibited good smoothness and non-stickiness [33].

Spreadability of Gel

The optimised LZL-loaded ethosomal gel formulation demonstrated a spreadability value of 7.9–0.52 g. cm/sec, while the conventional gel formulation displayed a spreadability value of 5.8–0.34 g. cm/sec, according to studies on spreadability [47]. This result aligns with the previously reported findings of a lipid gel encapsulating topical luliconazole. Increasing the polymer concentration decreases the spreadability of the gel due to higher viscosity.

In-vitro Drug Release

The LZL-solution (DR-LZL), LZL-conventional gel and LZL-ETs-g formulations' release patterns have been evaluated using the dialysis bag method. As per the results, LZL-solution (DR-LZL), demonstrated immediate first burst release, releasing roughly 55.0 ± 0.9% of LZL in just 2 h and 96.38 ± 0.8% in 4 h. The LZL-conventional gel shows 45 ± 1.35% in 12 h which is poor drug release profile, due to the dense gel and absence of penetration enhancer. The LZL-ETHs-gel's *in vitro* experiments showed a quick drug release of 20.9 ± 2.4% (contained within the carrier) in first 2 h, which was followed by a sustained release of 84.39 ± 1.5% for 12 h. The ETs gel showed sustained or delayed release following best fit as the Higuchi model with R^2 value is 0.9884. The LZL-ETs-gel shows promise for delivering luliconazole, as evidenced by the release pattern depicted in Fig. 7. Initially, there is a burst release attributed to the drug-enriched shell, followed by sustained release from the ethosome core. Drug diffusion occurs in two phases: across the gel structure and from reservoir vesicles, crucial for achieving both prolonged and burst release, essential for effective dermal application, ensuring sustained drug delivery, and enhanced penetration [29, 48].

In-vitro Anti-fungal Activity

In this study, the free drug solution, Optimized LZL-ETs-gel, and conventional gel are all tested against *Candida albicans*. The results showed that the free drug solution had the largest inhibition (22.7 mm), followed by the LZL-ETs-gel (19.4 mm), and the conventional gel (17.3 mm). The zone of inhibition shows in Fig. 8. This suggests that the ET formulation is more effective than the conventional formulation at inhibiting fungal growth. The results of this study are promising and suggest that the LZL-ETs-gel could be used as the formulation of choice for the treatment of the disease. Squalene-based ETs are a type of drug delivery system that can improve the solubility and bioavailability of the drug. This can lead to increased efficacy and reduced side effects.

Ex-vivo Permeation Study

The results of the *ex-vivo* permeation study in (Fig. 9) showed that the LZL-ETs-gel formulation was able to deliver the drug to the skin more effectively than the free drug solution or the conventional formulation. The lipid-based LZL-ETs-gel formulation, enriched with squalene, enhances drug penetration through the skin by increasing

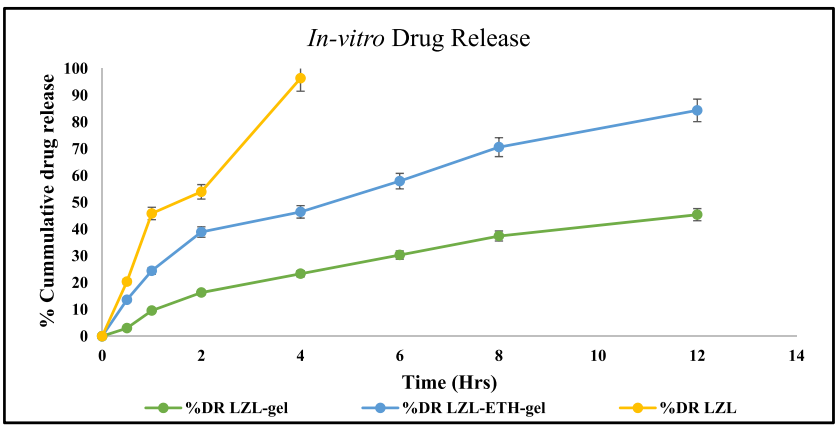

Fig. 7 *In-vitro* drug release of free drug solution, Optimized ETs-gel, and LZL-conventional gel

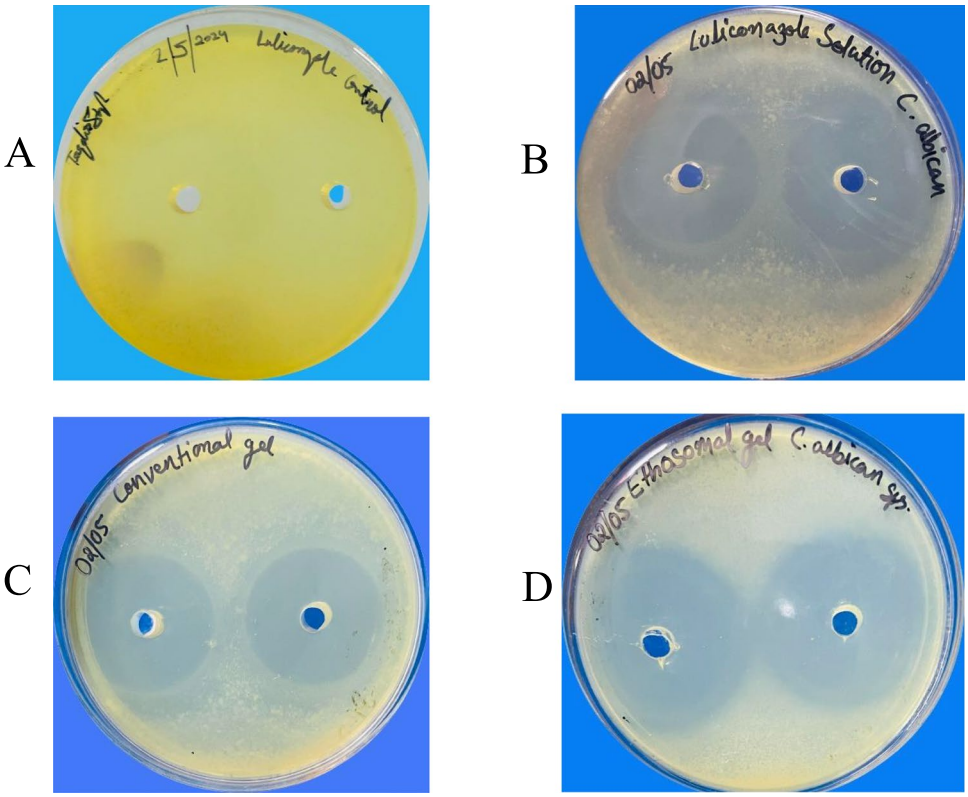

Fig. 8 shows that the **A** normal Control, **B** LZL- solution, **C** LZL-conventional gel, **D** LZL–ETs-gel. Zone of inhibition of free drug (LZL-solution), optimized LZL-ETs-gel, and conventional gel against Candida albicans. The free drug showed the highest antifungal activity, followed by LZL-ETs-gel and conventional gel, indicating improved efficacy of the ETs formulation

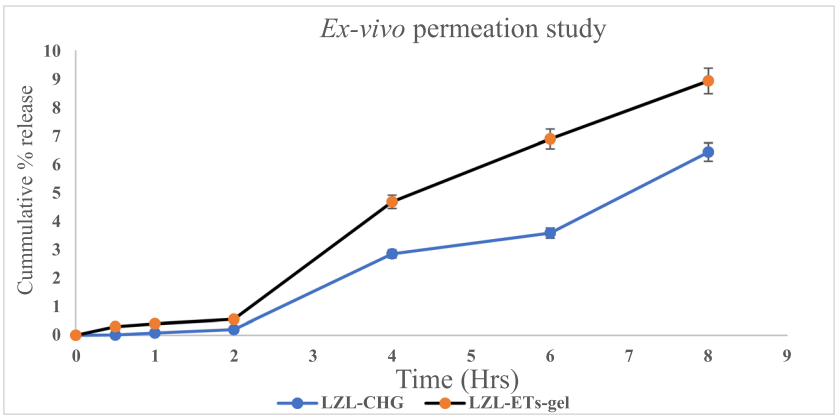

Fig. 9 *Ex vivo* permeation study cumulative % release SD < 5%

drug solubility in ethosomes and potentially disrupting the skin's lipid bilayer. This formulation is suggested to be more effective than free drug solution or conventional formulations, allowing for higher drug concentrations in the skin. The drug permeability of LZL-conventional gel and LZL-ETs-gel through pig skin was 0.20 ± 0.01% and 0.60 ± 0.02% at 2 h, respectively, 9.16 ± 0.70% and 6.42 ± 0.28% during 8 h of the study. LZL-ETs-gel retained a higher concentration of drug in the skin layer after 8 h. within 8 h, LZL-conventional gel and LZL-ETs-gel had drug retention rates of 45.74 ± 0.84% and 75.30 ± 1.37%, respectively (Fig. 10). The study showed that the ethosomes formulation had a higher proportion of drug deposition than the ordinary drug-containing gel. The results show that nano-vesicular components mixed into the gel can exert depot effect by reaching deeper into the dermal layer. Furthermore, the ethosomal coating allows for easier reach into cells and liquid lipid squalene which help to retain a high percentage of drug in skin, because the addition of squalene in ethosomal formulations restores lipid content on sebum. It enhances drug transfer through skin layers via partitioning, increase moisture, and prolongs retention in the dermis. This squalene based ethosomal gel of Luliconazole show better localized effect and compared to the conventional gel formulation [38, 49].

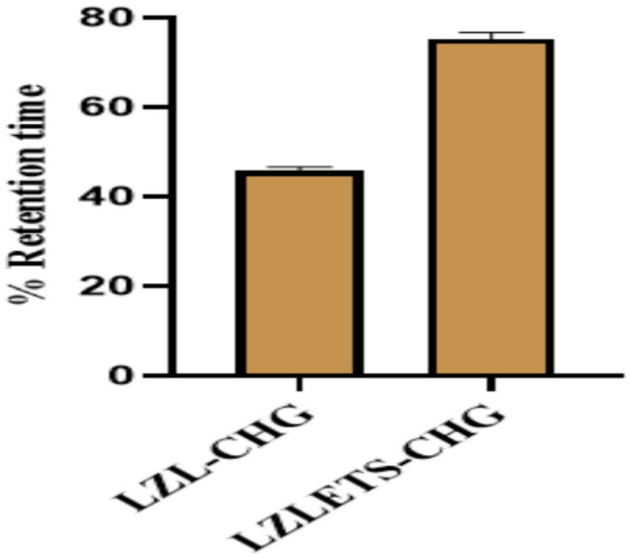

Fig. 10 Skin deposition study

In-vivo Anti-fungal Activity

The *in vivo* study utilized a *Candida albicans*-induced mycosis model to gain insights into the pharmacodynamic effects of the formulation. The growth and behaviour of the strain differ significantly inside living organisms compared to outside, complicating the assessment of drug activity solely through *in vitro* experiments. Therefore, this study aids in accurately predicting the antifungal efficacy of prepared formulations of LZL-ETs-gel and comparing them with its conventional formulation. *In vivo* infections in rats were confirmed through microbiological assessment of skin scraping samples obtained from the infected animals under investigation. Figure 11 (B, C, D). The results of study showed that the LZL-ETs-gel was more effective than the conventional gel reduced the growth of fungus. This is allowed the drug to reach higher concentration in the skin, which is necessary for effective treatment of *Candida albican* infection. The results of study shows that the LZL-ETs-gel formulation a more effective and safer way to treat dermatophytosis than the conventional formulation of drug. The LZL-ETs-gel formulation enhances penetration and prolongs retention time, as demonstrated in *ex-vivo* studies. Moreover, the ethosomal gel does not induce side effects such as skin irritation or allergic reactions[33].

Histopathology Study Histopathological evaluation Fig. 12 of skin samples were conducted using H&E staining. Histopathological evaluation using H&E staining (Fig. 12) of rat skin samples revealed distinct layers in control skin, including the stratum corneum, stratum granulosum, stratum spinosum, and stratum basale, with intact structures like hair follicles, sweat glands, sebaceous glands, and dermal

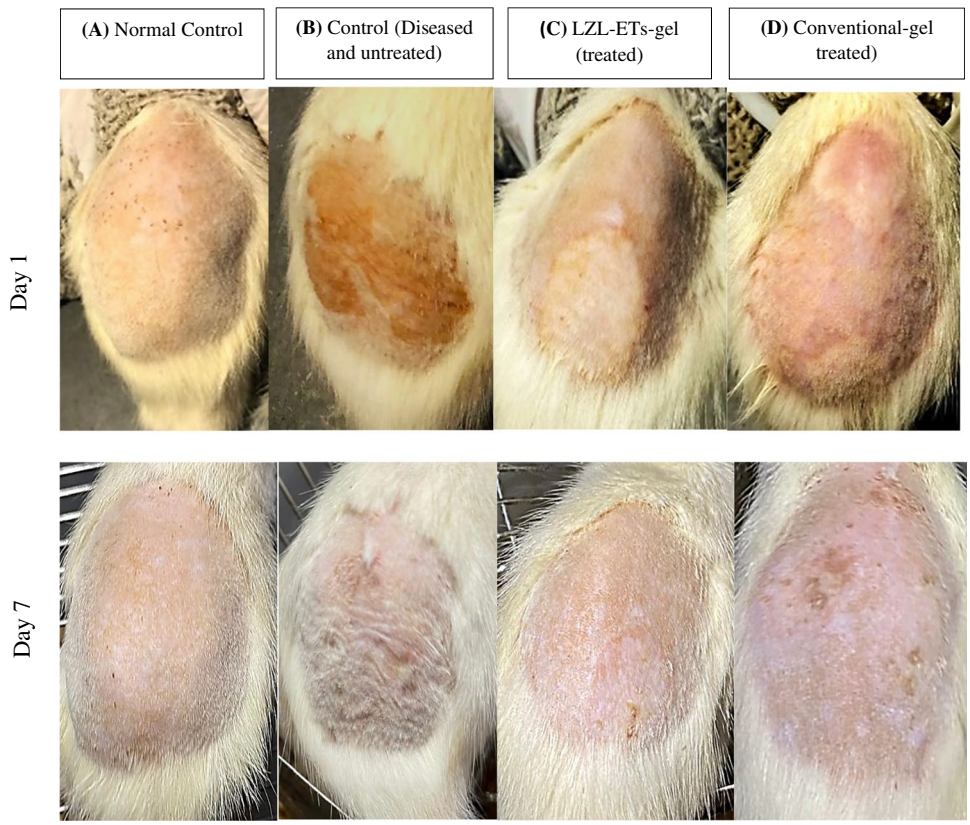

Fig. 11 Photographic images of rat show **A**)normal control, which is uninfected, **B** Control (infected and untreated), **C** and **D** shown before and after treatment *in vivo* anti-fungal activity of optimized LZL-ETs-gel and Conventional gel against Candida albicans after 7 days

papillae. (B) Group Infected, untreated skin exhibited increased epidermal thickness, hyperkeratosis, congestion, degeneration, extensive necrosis, and candidal spores in the dermis. The (C) group treated with optimized ethosomal gel showed minimal fungal spores, significant skin recovery with a well-defined epidermis, reduced inflammation, and edema. In contrast, the conventional gel-treated group (D) displayed fungal hyphae and spores in the epidermis and

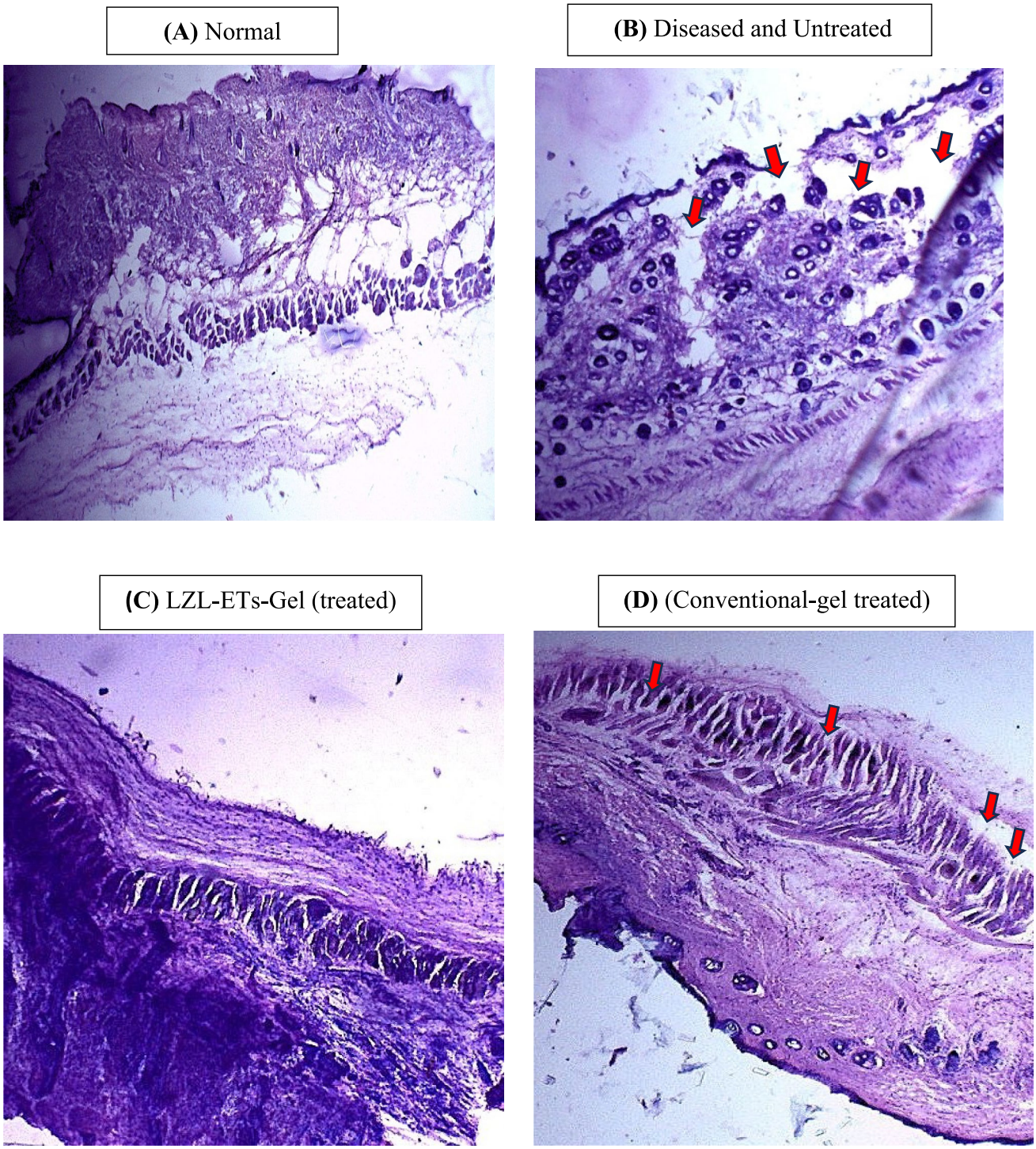

Fig. 12 Histopathological examination showed that the **A** control group which is not infected with diseased **B** diseased and untreated group of animals exhibited skin congestion. **C** skin treated with LZL-ETs-gel, showing better improvement in skin structure as compare to conventional treated gel, **D** group treated with conventional gel, which shows spores in epidermis and dermis

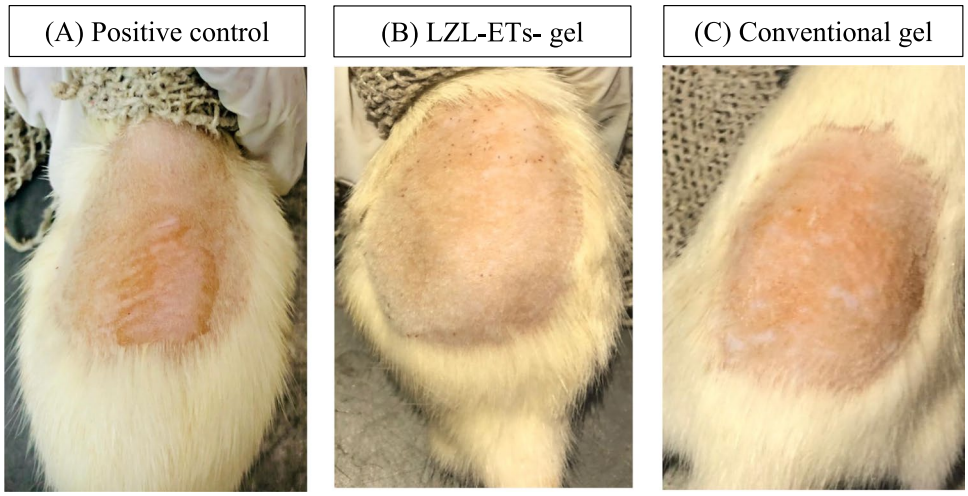

Fig. 13 Skin irritation assessment in Wistar rats following topical application of formulations over 4 days. The figure shows representative images of rat dorsal skin treated with **A** formalin solution (positive control), **B** conventional gel formulation, and **C** LZL-ETs-gel formulation. Formalin-treated rats exhibited visible erythema and edema, indicating significant skin irritation. In contrast, rats treated with both the conventional gel and ETs gel showed no signs of irritation, resulting in the formulations being skin compatible

dermis. Overall, LZL-ETs-gel demonstrated dermatological tolerance and safety for topical use. [33, 38]. The overall result showed that LZL-ETs-gel remained in the appropriate limits for dermatological tolerance and was considered safe for topical usage.

Skin Irritation Studies

Skin irritation assessments were carried out in Wistar rats to determine the potential for irritation from a conventional formulation and ethosomes in comparison to a positive control using formalin solution. The medications were applied twice each day to the rat's shaved dorsal region. The animals were observed for signs of cutaneous discomfort for four days. The formalin-treated group exhibited clear signs of skin irritation, with all animals showing grade 3 to 4 irritation, characterized by fiery redness and swelling (erythema and edema), indicating significant dermal toxicity. In contrast, rats treated with both the conventional gel and the ethosomal formulation showed no visible signs of erythema or edema, corresponding to an irritation score of 0 in all animals throughout the observation period (Shown in Fig. 13). This is in acute contrast to the results obtained with formalin solution, a well-known skin irritant. and ETs are non-irritating to the skin of the Wistar rats. The presence of biodegradable lipid squalene lowers the possibility of toxicity [35, 44].

Conclusion

The study demonstrates the significant potential of a squalene based ethosomal gel enhancing skin penetration, moisture retention, and localized drug delivery efficacy against moderate to severe fungal infections. To attain specified key quality attributes (CQAs) in novel formulations, the LZL-ETs drug delivery system was developed and optimized with the Box-Behnken design method. Major material characteristics were changed in 17 formulations based on predictions generated by Design Expert software (version 13), including phospholipid amount, squalene, and ethanol. Using similar software, vesicle size, entrapment efficiency, and PDI values were then measured and examined. The spherical shape of the ethosomes, with their uniform size as well as distribution, has been demonstrated by TEM images. The *ex vivo* skin permeation and retention studies showed significantly enhanced skin penetration and deposition with the nano-formulation gel. Skin irritation assessments conducted on rat skin indicated the absence of erythema. *In-vivo* antifungal activity experiments demonstrated that the novel LZL-ETs-gel formulation accelerated recovery in infected rats effectively. Consequently, LZL Ethosomal gels represent a promising formulation to maximize antifungal effectiveness against *Candida albicans* skin infections, potentially improving patient compliance and treatment outcomes.

Acknowledgements Declared none

Author Contributions **Taqdir Singh:** Data curation, Writing- original draft. **Akash Vikal:** Literature review and analysis. **Preeti Patel & Ghanshyam Das Gupta:** Formal analysis and language editing. **Shubham Thakur:** Investigation. **Balak Das Kurmi:** Conceptualization and supervision.

Funding Author is thankful to Indian Council of Medical Research (ICMR), New Delhi, India for providing financial assistance in the form of ICMR Adhoc Research Project. (File No.: 5/3/8/62/2020-ITR; IRIS ID:2020–3391).

Declarations

Consent for publication Not applicable.

Conflict of interest No conflict of interest was found.

Animal Experiments The protocol was approved by the Institutional Animal Ethics Committee (IAEC) of ISF College of Pharmacy (ISFCP/IAEC/CCSEA/Meeting No: 05/2024/Protocol No. 41).

References

1. Seth D, et al. Global burden of skin disease: inequities and innovations. Curr Dermatol Rep. 2017;6:204–10.
2. Kühbacher A, Burger-Kentischer A, Rupp S. Interaction of *Candida* species with the skin. Microorganisms. 2017;5(2):32.
3. Howell SA. Dermatopathology and the diagnosis of fungal infections. Br J Biomed Sci. 2023;80:11314.
4. Bongomin F, et al. Global and multi-national prevalence of fungal diseases-estimate precision. J Fungi. 2017. https://doi.org/10.3390/jof3040057.
5. Lionakis MS, Drummond RA, Hohl TM. Immune responses to human fungal pathogens and therapeutic prospects. Nat Rev Immunol. 2023;23(7):433–52.
6. Douglas AP, et al. Outbreaks of fungal infections in hospitals: epidemiology, detection, and management. J Fungi. 2023. https://doi.org/10.3390/jof9111059.
7. Reddy GKK, Padmavathi AR, Nancharaiah YV. Fungal infections: pathogenesis, antifungals and alternate treatment approaches. Curr Res Microb Sci. 2022;3:100137.
8. Burstein VL, et al. Skin immunity to dermatophytes: from experimental infection models to human disease. Front Immunol. 2020;11:605644.
9. Moskaluk AE, VandeWoude S. Current topics in dermatophyte classification and clinical diagnosis. Pathogens. 2022. https://doi.org/10.3390/pathogens11090957.
10. Bojang E, et al. Immune sensing of *Candida albicans*. J Fungi. 2021;7(2):119.
11. Chen L, et al. Confronting antifungal resistance, tolerance, and persistence: advances in drug target discovery and delivery systems. Adv Drug Deliv Rev. 2023. https://doi.org/10.1016/j.addr.2023.115007.
12. Wall G, Lopez-Ribot JL. Current antimycotics, new prospects, and future approaches to antifungal therapy. Antibiotics. 2020;9(8):445.
13. Teixeira MM, et al. New antifungal agents with azole moieties. Pharmaceuticals. 2022;15(11):1427.
14. Linder KA, Kauffman CA, Miceli MH. Blastomycosis: a review of mycological and clinical aspects. J Fungi. 2023;9(1):117.
15. Gupta AK, Versteeg SG, Shear NH. Onychomycosis in the 21st century: an update on diagnosis, epidemiology, and treatment. J Cutan Med Surg. 2017;21(6):525–39.
16. Garg AK, et al. Solubility enhancement, formulation development and antifungal activity of luliconazole niosomal gel-based system. J Biomater Sci Polym Ed. 2021;32(8):1009–23.
17. Khanna D, Bharti S. Luliconazole for the treatment of fungal infections: an evidence-based review. Core Evid. 2014;9:113–24.
18. Babu CK, et al. Luliconazole topical dermal drug delivery for superficial fungal infections: penetration hurdles and role of functional nanomaterials. Curr Pharm Des. 2022;28(20):1611–20.
19. Mishra AK, et al. Chemistry and pharmacology of luliconazole (imidazole derivative): a novel bioactive compound to treat fungal infection-a mini review. Curr Bioact Compd. 2019;15(6):602–9.
20. Garg V, et al. Ethosomes and transfersomes: principles, perspectives and practices. Curr Drug Deliv. 2017;14(5):613–33.
21. Sharma A, et al. Squalene integrated NLC based gel of tamoxifen citrate for efficient treatment of psoriasis: a preclinical investigation. J Drug Deliv Sci Technol. 2020;56:101568.
22. Paiva-Santos AC, et al. Ethosomes as nanocarriers for the development of skin delivery formulations. Pharm Res. 2021;38(6):947–70.
23. Chauhan N, et al. Ethosomes: a novel drug carrier. Ann Med Surg. 2022;82:104595.
24. Aljohani AA, et al. Binary ethosomes for the enhanced topical delivery and antifungal efficacy of ketoconazole. Open Nano. 2023;11:100145.
25. Verma P, Pathak K. Therapeutic and cosmeceutical potential of ethosomes: an overview. J Adv Pharm Technol Res. 2010;1(3):274–82.
26. Almuqbil RM, Aldhubiab B. Ethosome-based transdermal drug delivery: its structural components, preparation techniques, and therapeutic applications across metabolic, chronic, and oncological conditions. Pharmaceutics. 2025. https://doi.org/10.3390/pharmaceutics17050583.
27. Kumar M, Shanthi N, Mahato AK. Qualitative and quantitative methods for determination of drug luliconazole. International Journal of Research in Advent Technology. 2018;6(10):2321–9637.
28. Ondieki ASK, Rathore KS, Development and characterization of topical gel containing deep eutectic mixture of luliconazole for topical drug delivery system. Methods. 2023;10(4):294–302.
29. Kumar M, et al. Preparation of luliconazole nanocrystals loaded hydrogel for improvement of dissolution and antifungal activity. Heliyon. 2019. https://doi.org/10.1016/j.heliyon.2019.e01688.
30. Yang J, et al. Development of a luliconazole nanoemulsion as a prospective ophthalmic delivery system for the treatment of fungal keratitis: in vitro and in vivo evaluation. Pharmaceutics. 2022;14(10):2052.
31. Bhanu P, Sundararajan R. Spectrophotometric determination of Luliconazole in bulk and pharmaceutical dosage form. Res J Pharm Technol. 2020;13(2):928–32.
32. Malviya N, Prabakaran A, Alexander A. Comparative study on ethosomes and transferosomes for enhancing skin permeability of sinapic acid. J Mol Liq. 2023;383:122098.
33. Kaur M, Singh K, Jain SK. Luliconazole vesicular based gel formulations for its enhanced topical delivery. J Liposome Res. 2020;30(4):388–406.
34. Baghel S, et al. Luliconazole-loaded nanostructured lipid carriers for topical treatment of superficial tinea infections. Dermatol Ther. 2020;33(6):e13959.
35. Alhakamy NA, et al. Development, optimization, and evaluation of luliconazole nanoemulgel for the treatment of fungal infection. J Chem. 2021;2021(1):4942659.
36. Giri Y, et al. Development of microemulgel formulations with varied permeation enhancers for transungual delivery of luliconazole in onychomycosis management. Colloids Surf, B. 2024;234:113718.
37. Koga H, et al. In vitro antifungal activities of luliconazole, a new topical imidazole. Med Mycol. 2009;47(6):640–7.
38. Singh G, Narang RK. Quality by design assisted development of Luliconazole transethosomes in gel for the management of *Candida albicans* infection. Assay Drug Dev Technol. 2024;22(1):1–17.
39. Bhargav E, Reddy YP, Koteshwara KB. Development and optimization of luliconazole nanostructured lipid carriers based gel by quality by design its skin distribution studies, dermatokinetic modeling & in-vitro and ex-vivo correlation. Curr Drug Deliv. 2021;18(7):1041–53.
40. Alhakamy NA, et al. Retracted: optimized Icariin phytosomes exhibit enhanced cytotoxicity and apoptosis-inducing activities in ovarian cancer cells. Pharmaceutics. 2020;12(4):346.
41. Mishra S, Gupta RA. Formulation and evaluation of niosomal gel of antifungal luliconazole. J Drug Deliv Ther. 2022;12(6-S):47–54.
42. Mahmood A, et al. Luliconazole loaded lyotropic liquid crystalline nanoparticles for topical delivery: QbD driven optimization, in-vitro characterization and dermatokinetic assessment. Chem Phys Lipids. 2021;234:105028.
43. Sinhal APS, Wagh RDW, Formulation and Evaluation of Lipid-Based Nano Formulation of Luliconazole. 2023.

44. Singh G, Narang RK. Polymeric micelle gel with luliconazole: in vivo efficacy against cutaneous candidiasis in Wistar rats. Naunyn-Schmiedeberg's Arch Pharmacol. 2024;397:7001–7015.
45. Aldawsari MF, Alam A, Imran M. Rutin-loaded transethosomal gel for topical application: a comprehensive analysis of skin permeation and antimicrobial efficacy. ACS Omega. 2024. https://doi.org/10.1021/acsomega.4c01718.
46. Zhai Y, et al. Ethosomes for skin delivery of ropivacaine: preparation, characterization and ex vivo penetration properties. J Liposome Res. 2015;25(4):316–24.
47. Kumari S, et al. Development of soft luliconazole invasomes gel for effective transdermal delivery: optimization to in-vivo antifungal activity. Gels. 2023;9(8):626.
48. Yallavula J, Mandava K, Madhav V. Design and evaluation of topical gel containing solid-lipid nanoparticles loaded with luliconazole. International Journal of Pharmacy Research & Technology (IJPRT). 2023;13(2):52–64.
49. Mahmood A, et al. Dermatokinetic assessment of luliconazole-loaded nanostructured lipid carriers (NLCs) for topical delivery: qbd-driven design, optimization, and in vitro and ex vivo evaluations. Drug Deliv Transl Res. 2022;12(5):1118–35.